RSC Advances

PAPER

View Article Online
View Journal | View Issue

Cite this: *RSC Adv.*, 2020, **10**, 29202

Active biodegradable packaging films modified with grape seeds lignin†

Pavel Vostrejs,[a] Dana Adamcová,[b] Magdalena Daria Vaverková,[bc] Vojtech Enev,[d] Michal Kalina,[d] Michal Machovsky,[e] Markéta Šourková,[b] Ivana Marova[a] and Adriana Kovalcik *[a]

Biodegradable packaging materials represent one possible solution for how to reduce the negative environmental impact of plastics. The main idea of this work was to investigate the possibility of utilizing grape seed lignin for the modification of polyhydroxyalkanoates with the use of its antioxidant capacity in packaging films. For this purpose, polymeric films based on the blend of high crystalline poly(3-hydroxybutyrate) (PHB) and amorphous polyhydroxyalkanoate (PHA) were prepared. PHB/PHA films displayed Young modulus of 240 MPa, tensile strength at a maximum of 6.6 MPa and elongation at break of 95.2%. The physical properties of PHB/PHA films were modified by the addition of 1–10 wt% of grape seeds lignin (GS-L). GS-L lignin showed a high antioxidant capacity: 238 milligrams of Trolox equivalents were equal to one gram of grape seeds lignin. The incorporation of grape seeds lignin into PHB/PHA films positively influenced their gas barrier properties, antioxidant activity and biodegradability. The values of oxygen and carbon dioxide transition rate of PHB/PHA with 1 wt% of GS-L were 7.3 and 36.3 cm^3 m^{-2} 24 h 0.1 MPa, respectively. The inhibition percentage of the ABTS radical determined in PHB/PHA/GS-L was in the range of 29.2% to 100% depending on the lignin concentration. The biodegradability test carried out under controlled composting environment for 90 days showed that the PHB/PHA film with 50 w/w% of amorphous PHA reached the degradability degree of 68.8% being about 26.6% higher decomposition than in the case of neat high crystalline PHB film. The degradability degree of PHA films in compost within the tested period reflected the modification of the semi-crystalline character and varied with the incorporated lignin. From the toxicological point of view, the composts obtained after biodegradation of PHA films proved the non-toxicity of PHB/PHA/GS-L materials and its degradation products showed a positive effect on white mustard (*Sinapis alba* L.) seeds germination.

Received 6th May 2020
Accepted 21st July 2020

DOI: 10.1039/d0ra04074f

rsc.li/rsc-advances

1. Introduction

The challenge to our society is to decrease the amount of durable and non-biodegradable packaging. Currently, the sustainability for the production and consumption of goods has begun to be a driving force in many areas but mainly in the packaging industry where an increasing number of companies (*e.g.*, Unilever's Carte d'Or, Nestlé, Nature's Way) started to relaunch "eco-friendly" material alternatives such as recyclable materials, bioplastics and paper-based packaging.[1,2] The challenge is to offer non-toxic, sustainable, ideally (bio) degradable and low-cost materials meeting the criteria on physical appearance, barrier properties and thermo-mechanical stability.

Polyhydroxyalkanoates (PHAs) belong to biobased, biocompatible and biodegradable polymers produced by various prokaryotes in the form of intracellular granules mainly as carbon storage compounds. PHAs have the potential to substitute non-biodegradable petrochemical polymers. They are a large, diverse group of biological polyesters having properties in the range from thermoplastic to elastomers.[3] They are commercially available with applications in pharmacy, medicine, cosmetics and functional materials for niche applications.[4–8] Poly(3-hydroxybutyrate) (PHB) is the most reviewed and most widely used within the PHAs. The reason is that biosynthesis of PHB compared to the biosynthesis of other types of PHAs is simpler and brings at least 50 times higher polymer yields. Depending on the type of bacteria strain and cultivation

[a]*Department of Food Chemistry and Biotechnology, Faculty of Chemistry, Brno University of Technology, Purkynova 118, 612 00 Brno, Czech Republic. E-mail: kovalcik@fch.vut.cz*

[b]*Department of Applied and Landscape Ecology, Faculty of AgriSciences, Mendel University in Brno, Zemědělská 1, 613 00 Brno, Czech Republic*

[c]*Institute of Civil Engineering, Warsaw University of Life Sciences – SGGW, Nowoursynowska 159m, 02 776 Warsaw, Poland*

[d]*Department of Physical and Applied Chemistry, Faculty of Chemistry, Brno University of Technology, Purkynova 118, 612 00 Brno, Czech Republic*

[e]*Centre of Polymer Systems, Tomas Bata University in Zlín, Třída Tomáše Bati 5678, 760 01 Zlin, Czech Republic*

† Electronic supplementary information (ESI) available. See DOI: 10.1039/d0ra04074f

conditions, the PHB yields can be about 89–149 g of PHB per litre of cultivation medium. Nevertheless, the biosynthesis of copolymers, *e.g.*, poly(3-hydroxybutyrate-*co*-3-hydroxyvalerate) (PHBV), results in yields being about 6.5 to 11.7 g l^{-1}.[9,10] The possible application of PHB depends on product requirements. For products requiring high agility and flexibility, PHB's use is inappropriate due to its high crystallinity and brittleness. It has been found that the brittleness of PHB products increases over time due to secondary crystallization and physical ageing. PHB is a semi-crystalline polymer and the ratio of amorphous and crystalline moieties significantly affects its mechanical properties. Reducing crystallinity and faster crystallization *via* nucleation contribute to the improvement of the mechanical properties of PHB.[11] The plasticization is one of the methods on how to decrease the crystallinity of PHB and reach a higher ductility of PHB materials.[12,13] Another method for decreasing fragility is the blending of PHB with flexible polymers (*e.g.*, poly(caprolactone)).[14]

The purpose of this study is (1) to investigate the thermal properties, mechanical properties and gas permeability of high crystalline PHB blended with amorphous PHA, (2) to assess the effect of grape seeds lignin incorporation on thermal properties, mechanical properties of PHB/PHA blends and (3) to determine the antioxidant effect of grape seeds lignin incorporated in PHB/PHA films. The hypothesis was that amorphous PHA with rubber-like mechanical behaviour would modify the crystallization behaviour of PHB. Moreover, lignin isolated from grape seeds should possess high antioxidant activity, which would be beneficial for food packaging applications.[15] Polymeric materials are susceptible to be attacked by molecular oxygen through radical reactions. To eliminate the oxidation degradation, various antioxidants, *e.g.*, hindered phenols, are used for plastic packaging materials.[16] Lignins are biopolymers naturally present in plant tissues and have phenolic character. They help plants to fight against different chemical, biological and mechanical stresses mainly by scavenging of radical species. Lignins do not have a uniform structure and their antioxidant activity vary with their chemical composition and molecular weight. Practically, every type of lignin is unique and its chemical and physical properties depend on the source of origin, extraction and treatment methodology.[17] The expectations followed in this investigation were that sulfur-free grape seeds lignin might be an excellent antioxidant for PHB/PHA blend and could contribute to lower gas permeability of final films.

A further objective of this work was to assess the compostability of PHB and PHB/PHA films with grape seeds lignin. PHB decomposes under favourable conditions in compost.[18,19] To the best of our knowledge, the effect of lignin on composting and phytotoxicity of PHB blended with the amorphous PHA has not yet been reported.

2. Materials and methods

2.1. Materials

Poly(3-hydroxybutyrate) (PHB), Hydal with a weight-average molecular mass (M_w) of 350.2 ± 3.4 kDa and polydispersity ($Đ$) of 1.17 ± 0.03 was kindly supplied by the Nafigate Corporation, Prague, Czech Republic. Amorphous polyhydroxyalkanoate (PHA), Mirel grade with a weight average molecular weight of 188.6 ± 1.9 kDa and polydispersity of 1.24 ± 0.01 was obtained from former Metabolix (Cambridge, MA, USA). Molecular weight properties of PHB and amorphous PHA were determined within this study.

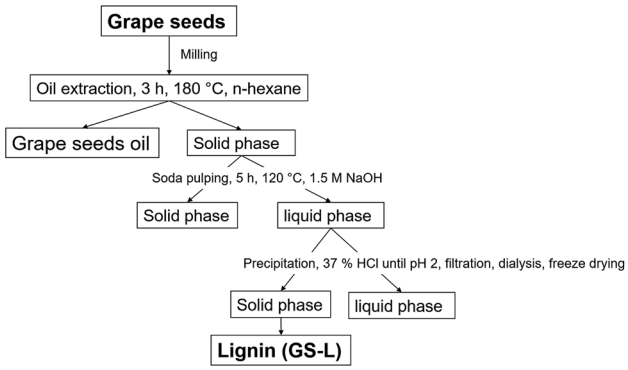

Fig. 1 The used approach to extract lignin from grape seeds.

Table 1 Composition of PHA films

Sample	PHB (wt%)	PHA (wt%)	Grape seed lignin (wt%)	Joncryl (wt%)
PHB	100	—	—	—
PHB/PHA	50	50	—	2
PHB/PHA_1_GS-L	48.5	48.5	1	2
PHB/PHA_5_GS-L	46.5	46.5	5	2
PHB/PHA_10_GS-L	44.0	44.0	10	2

Joncryl® ADR 4468 was used as a polymeric chain extender and kindly supplied by the BASF Corporation, USA. This multifunctional reactive polymer is registered as an additive for food contact applications.[20] Sodium hydroxide (≥99%), chloroform (ROTIPURAN ≥ 99% p.a.), *n*-hexane (ROTISOLV ≥ 99%) and chloroform (ROTISOLV HPLC) were purchased from Carl Roth, Germany. Hydrochloric acid (37%), pyridine (99.9%), acetic anhydride (98%), ABTS (2,2′-azino-bis(ethylbenzthiazoline-6-sulfonic acid)) and potassium persulfate were obtained from Sigma-Aldrich, Germany.

Grape seeds were collected from winery Vavricek (Brezi u Mikulova, Czechia) during fall 2018, including two white varieties Green Veltliner Green and Sauvignon Blanc. The seeds were separated from dried pomace (40 °C for five days). The seeds were vacuum packaged and stored until the extracting process. Firstly, oil was extracted from seeds in *n*-hexane using Soxtherm (Gerhardt, Germany) at 180 °C for 3 hours. Consequently, lignin (GS-L) was isolated from the oil-free solid phase by soda pulping (see Fig. 1) by precipitation with 37% hydrochloric acid until it had reached pH 2. The precipitate was filtered and dialyzed in fresh distilled water for 7 days until pH 7 and subsequently freeze-dried. For the dialysis of lignin was used the dialysis membrane (Membra-Cel – Viscose, Carl Roth,

Karlsruhe, Germany) with the pores of 1.5–2.0 nm. Klason lignin and acid soluble lignin were determined, according to Tappi methods.[20,21]

PHB, PHB/PHA and PHB/PHA/GS-L films were prepared by solution casting in chloroform according to Wu *et al.*[22] In total, 1 g of materials (detailed composition is shown in Table 1) was dissolved in hot chloroform and poured onto Petri dishes. First, the dishes were kept at room temperature for three days. After chloroform evaporation, the films were peeled out from dishes. The polymer films were vacuum dried at 25 °C for one hour to remove chloroform completely.

2.2. Analytical methods

The elemental composition of lignins was determined using a CHNS analyzer Euro Vector EA 3000. Samples (~0.5–1.5 mg) were packed in tin capsules in the oven for combustion at 980 °C using pure oxygen as the combustion gas and pure helium as the carrier gas. All elements were determined by a thermal conductivity detector (TCD). The calibration curves for C, H, N, S were obtained using a reference standard sample sulphanilamide. The percentage of oxygen content was calculated by difference and the values obtained were corrected for ash and moisture content.

Fourier transform infrared spectroscopy (FTIR) spectrum of lignin was obtained employing a Diffuse Reflectance Infrared Fourier Transform (DRIFT) technique using a Nicolet iS50 spectrometer (Thermo Fisher Scientific, Waltham, USA). Approximately 2 mg of powdered lignin was homogenized with 200 mg of KBr and then transferred to the sample holder cup of the diffuse reflectance accessory. DRIFT spectra were recorded over the range 4000–400 cm^{-1} at 8 cm^{-1} resolutions and represented an average of 512 scans. The KBr infrared grade spectrum was used as the background for DRIFT measurement. Raw absorption DRIFT spectrum was evaluated with no artificial processing (*e.g.* baseline corrections and atmospheric suppression).

The molecular weight and polydispersity of the grape seed lignin isolated from grape seeds and commercial PHB, PHA samples was determined by Size Exclusion Chromatography (SEC, Infinity 1260, Agilent Technologies, USA) coupled to a Multiangle Laser Light Scattering detection (MALLS, Dawn Heleos II, Wyatt Technology, USA) and a Differential Refractometry (dRI, Optilab T-rEX, Wyatt Technology, USA). To achieve the sufficient solubility of lignin in chloroform was executed by acetylation according to Glasser *et al.*[23] The samples were solubilized in HPLC-grade chloroform (4 mg ml^{-1}) overnight and filtered before analysis through a syringe filter (nylon membrane, pore size 0.45 μm). For the analysis, 100 μl of the sample was injected into a chromatographic system containing HPLC-grade chloroform (pre-filtered through 0.02 μm membrane filter). The used flow rate was 0.6 ml min^{-1}. The SEC separation was performed using a PL Gel MIXED-C column (300 × 75 mm, Agilent Technology, USA). In the case of acetylated lignin sample, the molecular weight ($M_{w_{app}}$ weight-average) and polydispersity ($Đ_{app}$), determined by ASTRA software (Wyatt Technology, version 6.1) using the value of the refractive index increment of lignin in chloroform (dn/dc = 0.165 ml g^{-1}),[24] represent a fitted result obtained from an extrapolation of measured data using exponential fitting model. This approach was used to correct the absorption and the fluorescence of lignin. Both these phenomena significantly influence the intensity of scattered light and can cause the undesirable overestimation of a molecular weight determined by MALLS detection.[25] In the case of the commercial PHA and PHB samples, M_w and $Đ$ were calculated by ASTRA software using the value of the refractive index increment of PHA/PHB in chloroform (dn/dc = 0.0334 ml g^{-1}), as was determined from the differential refractometer response assuming a 100% sample mass recovery from the column.

The total phenolic content and the hydroxyls content of the GS-L sample was determined by the Folin–Ciocalteau spectrophotometric method using gallic acid as reference. Lignin was dissolved in dimethyl sulfoxide. The detailed methodology is described by Gordobil and coworkers.[26] The total phenolic contents were expressed as gallic acid equivalents (mg GAE per g lignin).[26]

The hydroxyls content was expressed according to the following formula:[26]

$$\mathrm{OH}\ (\%) = \frac{c_{\mathrm{GAE}}}{170.12 \times 100} \times 4 \times 17 \times \frac{1}{c_{\mathrm{lignin}}} \quad (1)$$

where, c_{GAE} is the concentration of gallic acid and c_{lignin} is the concentration of GS-L sample dissolved in DMSO.

The radical scavenging activity of grape seed lignin was determined using TEAC (Trolox Equivalent Antioxidant Capacity) assay according to Qazi *et al.*[27] Free radical scavenging activity of PHA films with lignin was examined by using ABTS radical scavenging assay.[28,29] This test is based on the ability of materials with free radical scavenging ability to scavenge the $ABTS^{\bullet+}$ radical cation, which was prepared by a reaction of 7 mM solution of ABTS in distilled water with 2.45 mM solution of potassium persulfate (incubation before using was 12 h in the dark). Prior to its use, the stock ABTS radical solution was diluted with UV ethanol to an absorbance of 0.7 ± 0.02 at 734 nm. Twenty millilitres of such prepared solution was poured in the vials with polymer films (surface area of about 2.5 cm^2 weights about 0.0369 g). Three parallel measurements were performed. The absorbance of solutions at the beginning and after 60 min of conditioning at 30 °C have been determined. The antioxidant capacity of lignin incorporated in PHB/PHA films was calculated as inhibition percentage (IP) of the radical species (IP, %) based on the absorbance changes in PHB/PHA films with and without lignin after 60 minutes:[30]

$$\mathrm{IP}\ (\%) = \frac{A_0 - A_1}{A_0} \times 100 \quad (2)$$

where, A_0 is the absorbance of PHB/PHA film without lignin and A_1 is the absorbance of PHB/PHA films with lignin after 60 minutes for $ABTS^{\bullet+}$ assay.

The data of antioxidant activity of lignin incorporated in PHB/PHA films were analyzed from the point of view of statistical significance by the analysis of variance employing Origin

(version Origin Pro 2018). The Tukey test's differences among mean values were processed at a level of significance of $p < 0.05$.

DSC experiments were performed using a DSC 8000 (PerkinElmer) under a nitrogen atmosphere. The calibration of DSC was accomplished with high purity indium. Samples of about 10 mg were hermetically sealed in aluminium pans. The samples were tested according to the non-isothermal protocol using the first heating–cooling-second heating cycle. The employed temperature ranges were heating from 25 °C to 190 °C, cooling from 190 °C to −20 °C and heating from −20 °C to 190 °C with heating/cooling rate of 10 °C min^{-1}. Melting temperature (T_m) and enthalpy of melting (ΔH_m) were determined from the endothermic peak. The crystallization temperature (T_c) and enthalpy of crystallization (ΔH_c) were measured from the exothermic peak.

Thermogravimetric analyses (TGA) experiments were performed by TGA Q50 (TA Instruments, USA) with an airflow of 30 ml min^{-1}. Approximately 5 mg of the sample was sealed in an aluminium crucible, heated from 25 °C to 400 °C with a heating rate of 10 °C min^{-1} and analyzed.

Mechanical properties of dumb-bell shape specimens cut from films were measured on an Instron 3365 (Instron, USA). The gauge length was 20 mm, and the thickness of the samples was 0.15 mm. The applied strain rate was 1 mm min^{-1}. The average E-modulus values, tensile stress at maximum (σ_{max}) and tensile strain at break (ε_B) were calculated from stress/strain plots of five specimens.

The morphology of films was investigated by thermionic emission scanning electron microscopy (ESEM) (VEGA II LMU, TESCAN). The microscope equipped with the S.E. detector was operated in high-vacuum mode at an acceleration voltage of 5 kV.

To analyse the lignin migration from the PHB/PHA films with the content of 5 wt% and 10% lignin were used (1) 10 wt% aqueous ethanol (simulate aqueous food products), and (2) 50 wt% aqueous ethanol (simulate fatty food products).[31] The methodology was used as follows: 0.1 g of the film was immersed in 20 ml 10 v/v% or 50 v/v% aqueous ethanol in test tubes and shaken at 50 rpm and room temperature. After eight days, the films were removed, the ethanol solution was allowed to evaporate, and the amount of lignin released was determined gravimetrically in dry tubes. The experiments were performed in three replicates. The amount of leached lignin was calculated by averaging three experimental runs.

Oxygen (O_2; purity of 99.9%) and carbon dioxide (CO_2, purity of 99%) permeability of PHA films (with a round diameter of 97 mm) were determined by VAC-V1 Gas Permeability Tester (Labthink). The gas flow was determined by monitoring the pressure as a function of time in calibrated volume connected to the downstream side of the polymer film. Gas transmission rate (GTR; [cm^3 m^{-2} 24 h 0.1 MPa]) was evaluated according to the following equation (ISO 2556):

$$\mathrm{GTR} = \frac{V_c}{R \times T \times p_a \times A} \times \frac{\mathrm{d}p}{\mathrm{d}t} \quad (3)$$

where V_c is the volume of the low-pressure side, T is the test temperature (thermodynamic temperature), p_a is the atmospheric environmental pressure (Pa), A is the active transmission area (in cm), dp/dt is the pressure variation at the low-pressure side per unit time after the transmission becomes stable, R is the gas constant.

Table 2 Description and characteristics of test samples[a]

Sample – description	m_0 (g)
PHB	1.47
PHB/PHA	1.60
PHB/PHA_1_GS-L	1.65
PHB/PHA_5_GS-L	1.69
PHB/PHA_10_GS-L	1.81
E – Reference (cellulose filter paper)	1.69

[a] m_0 – weight at the beginning of the experiment.

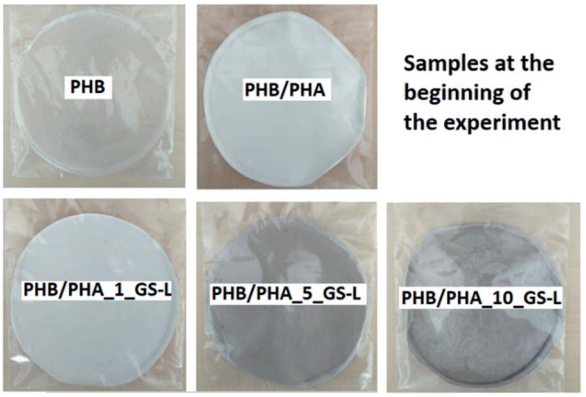

Fig. 2 PHB, PHB/PHA, PHB/PHA_1_GS-L, PHB/PHA_5_GS-L, and PHB/PHA_10_GS-L films at the beginning of composting.

2.3. Composting

The biodegradability of the prepared polymer films (Table 2) was assessed as per ČSN EN ISO 20200 and they were compared to biodegradable reference material (cellulose filter paper) under controlled composting conditions.

At the beginning of the experiment, the samples (Fig. 2) were weighed and their initial mass (m_0) was recorded. Samples were placed in testing containers of 180 × 180 mm, put in a compost reactor (300 × 200 × 100 mm) and mixed with a compost pile made of 40 w/w% sawdust, 30 w/w% biologically degradable waste, 10 w/w% compost, 10 w/w% starch and 5 w/w% sucrose. The reactors were equipped with a lid providing a tight seal to prevent excessive evaporation. The temperature was set at 58 °C; moisture was correlated by adding distilled water according to the requirements and aeration was switched at regular intervals to provide aerobic conditions.

Aeration inside the reactors was reached through the holes with a diameter of 5 mm at each side of the reactor (scheme of a composting experiment can be found in the ESI, see Fig. S1†). During the composting test, moisture, pH and temperature were controlled according to the schedule shown in Table 3.

At the end of the composting period (after 90 days) was each compost sample dried at 60 °C until a constant mass and sieved

Table 3 Controlling schedule applied during composting of PHA films

Time (days)	Activities
0	Preparation of reactors Weighing of reactors Temperature and pH measurement
1, 2, 3, 4, 5, 9, 10, 12, 14, 18, 20, 22, 24, 28, 30	Weighting of reactors Addition of water to restore 100 wt% of the initial mass Mixing and manual aeration Temperature and pH measurement
From day 31 to 45: twice a week	Weighing of reactors to control water mass Addition of water to restore 80 wt% of the initial mass Mixing and manual aeration Temperature and pH measurement
From day 46 to 90: twice a week	Weighing of reactors to control water mass Addition of water to restore 70 wt% of the initial mass. Temperature and pH measurement

through a 2 mm sieve. The sample pieces greater than 2 mm were weighted. The degradability degree (D) was calculated according to:[32]

$$D(\%) = \frac{m_0 - m_E}{m_0} \times 100 \quad (4)$$

where m_0 is the initial dry mass of tested film and m_E is the dry mass of tested film after composting and sieving.

2.4. Phytotoxicity experiment

The phytotoxicity of compost material resulting after 90 days of PHA film composting was determined by using a commercial toxicity bioassay – Phytotoxkit Test (Microbiotest, Nazareth, Belgium, Phytotoxkit™ 2004). The design of a phytotoxicity test can be found in the ESI, see Fig. S2.† The investigation of the phytotoxicity was based on the determination of germination and growth of white mustard (*Sinapis alba* L.) roots after 72 h of incubation at 25 °C in the soil with 5 wt% or 10 wt% of compost material received after biodegradation of PHA films.

The experiments were performed in three replicates. The Phytotoxkit test's principle is the measurement of changes in seed germination and the growth of young roots after incubation time. The length measurements of roots were analyzed using Image Tool 13.0 for Windows (UTHSCSA, San Antonio, USA). The per cent inhibition of seed germination and root growth inhibition (SGI) was calculated according to:[33]

$$\mathrm{SGI}\ (\%) = \frac{A - B}{A} \times 100 \quad (5)$$

where, A is average seed germination and root length determined in neat OECD soil and B is average seed germination and root length in the OECD soil with the compost received after PHA biodegradation. OECD soil with the composition of 74 wt% sand, 20 wt% kaolinite, 5 wt% peat and 1 wt% $CaCO_3$ was purchased from the MicroBioTests (Belgium).

3. Results and discussion

3.1. Lignin

The grape seeds are lignocellulosic materials with the unique high content of lignin. The Green Veltliner and Sauvignon Blanc seeds contained about 4.3 ± 0.2 w/v% of oil (extracted with *n*-hexane) and 40.2 wt% of lignin (total amount of lignin determined as a sum of Klason lignin and soluble acid lignin). Other authors also detected the considerable high amount of Klason lignin in grape seeds.[34,35] The grape seed lignin (GS-L) was isolated by the soda pulping method that enables the preparation of sulfur-free lignin. Some published works presented that sulfur-free lignins were more beneficial for the incorporation in polymers and often showed high antioxidant efficiency in plastic materials.[36–38]

However, unlike the mentioned literature, GS-L had a relatively higher molecular weight and contained high ash and nitrogen (Table 4). Contents of ash and nitrogen correspond to the natural presence of minerals and proteins in grape seeds.[32] The isolated GS-L had a molecular weight of 10.1 ± 0.8 kDa and polydispersity of 4.6 ± 0.6, respectively (Table 4 and S3†). The broad molecular weight distribution is typical for lignins isolated from annual plants.[39–41] Condensation reactions often occur during isolation procedures and contribute to the formation of high molecular weight lignins.[42]

The determined molecular weight is an apparent value ($M_{w_{app}}$) because it was obtained after the application of two correction procedures necessary for the elimination of lignin absorption and fluorescence from the MALL's data. As was already described by Zinovyev *et al.*,[25] in the case of lignin, both these phenomena represent significant issues causing the undesirable overestimation of measured M_w by MALLS technique, primarily if a red laser is used in MALLS (663.8 nm laser used in our MALLS). The absorption of the acetylated lignin sample was corrected by changing the light scattering intensity relation to the laser intensity of the forwarding monitor detector. At this point, the original and default MALLS setting used for the non-absorbing samples is the light scattering intensity relation to the laser intensity of the laser monitor

Table 4 Elemental composition and molecular properties of grape seeds lignin

	Elemental composition (wt%)							
Sample	C	H	N	S	O	Ash (wt%)	$M_{w_{app}}$ (kDa)	$Đ_{app}$ (−)
GS-L	61.6 ± 0.8	8.4 ± 0.2	2.9 ± 0.1	—	20.6 ± 0.1	6.5 ± 0.5	10.1 ± 0.8	4.6 ± 0.6

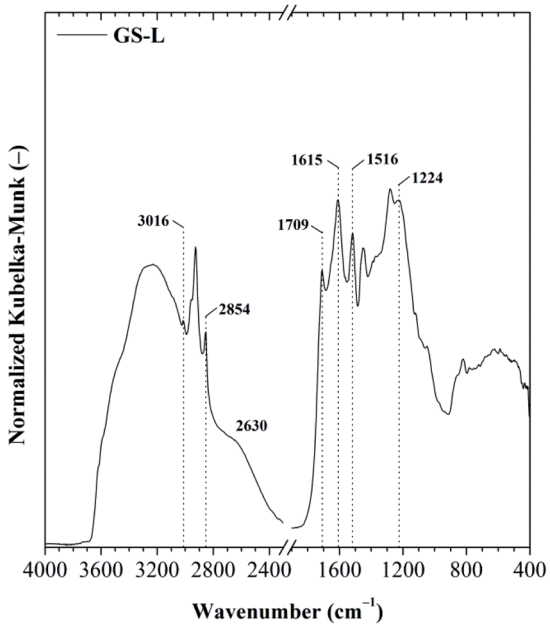

Fig. 3 ATR-IR spectrum of the grape seeds lignin (GS-L).

detector. The elimination of fluorescence from light scattering data is based on its minimal effect at the very beginning of the MALLS chromatogram where the scattered light dominates. With increasing elution time, fluorescence becomes increasingly prominent, resulting in an increasing overestimation of the determined molecular weight.[25] According to these findings, the data from the initial stages of MALL's chromatogram were fitted using the exponential model and extrapolated towards higher elution times resulting in corrected apparent values of $M_{w_{app}}$ and $Đ_{app}$. These results are in good correlation with the values of the molecular weight of lignin published in the literature.[40,43]

The total phenolic content for GS-L lignin was 313 ± 11 mg GAE per g lignin. Lignin contained ~12.5% of hydroxyls. The quantified $ABTS^{\bullet+}$ radical scavenging activity of grape seeds lignin was 238 ± 16 mg Trolox equivalents on one gram of lignin. The prominent radical scavenging activity of grape seeds lignin corresponded with its high total phenolic content and hydroxyl groups. However, the antioxidant activity depends also on the other factors. To reach high antioxidant activity the low molecular weight, narrow polydispersity and the absence of sulfur in lignin structure were found to be beneficial.[26,36–38] The structure of grape seeds lignin was determined by FTIR spectroscopy. Lignin is an aliphatic-aromatic polymer. The DRIFT spectrum of lignin showed several spectral features typical for lignin (Fig. 3). Lignin showed C–H stretching vibrations in the aromatic rings in the range of 3070–3010 cm^{-1}. Out-of-plane C–H deformation bands were found in the range of 900–820 cm^{-1}. The aliphatic chains were shown in the range of 3000–2800 cm^{-1}. The pronounced absorption bands at 2927 cm^{-1} and 2858 cm^{-1} were ascribed to asymmetric and symmetric C–H stretching in $–CH_2–$ groups. The deformation vibrations of the $–CH_2–$ and $–CH_3$ groups appeared at 1450 cm^{-1}. The carboxylic groups resulted from the O–H stretching vibrations of the hydrogen-bonded COOH of which forms dimers were indicated by the broad band centred at about 2630 cm^{-1}. Carboxylic groups' vibrations were also manifested by the presence of the typical intensive band 1709 cm^{-1}. The band centred at about ~1280 cm^{-1} was attributed to C–O stretching of carboxylic groups. Moreover, the O–H stretching of phenolic, alcoholic and carboxylic functional groups connected with an intermolecular hydrogen-bond was manifested by a band centred at 3240 cm^{-1}. The band at 1224 cm^{-1} was assigned to stretching C–O groups in phenolic –OH functional groups. The intensive absorption band at 1369 cm^{-1} indicated the C–H bending of methoxyl functional groups.

Other significant absorption bands typical for lignin resulting from skeletal vibrations of C=C stretching in aromatic rings were revealed at ~1615 ± 5 cm^{-1} and ~1508 cm^{-1}. The lignin FTIR spectrum was analyzed according to the literature.[44]

3.2. PHA films

3.2.1. FT-IR analysis of PHB, PHB/PHA and PHB/PHA/lignin films. The structural changes of PHB/PHA/GS-L blends were characterized by ATR-FTIR. The spectra provided signature bands represented by polyhydroxyalkanoates and grape seed lignin are shown in Fig. 4a and b. The detailed interpretation of the leading absorption bands of PHAs can be found in the literature.[45–47] Briefly, the crystalline regions are indicated by the sharp and intensive bands centred at about 1720 cm^{-1}, 1276 cm^{-1} and 1227 cm^{-1} resulting from the symmetric C=O and C–O stretching vibrations of the aliphatic esters. The absorption band located at 980 cm^{-1} was assigned to the skeletal C–C vibration mode that corresponds to the crystalline phase of PHAs. As expected, the intensities of these absorption bands were higher for neat PHB than in PHB/PHA films with or without lignin. The FTIR spectra proved that PHB is much more crystalline than PHB/PHA blends. In the PHB/PHA blends were well visible bands at 1176 cm^{-1} and 1130 cm^{-1} known to arise from the amorphous phase. These peaks are ascribed to

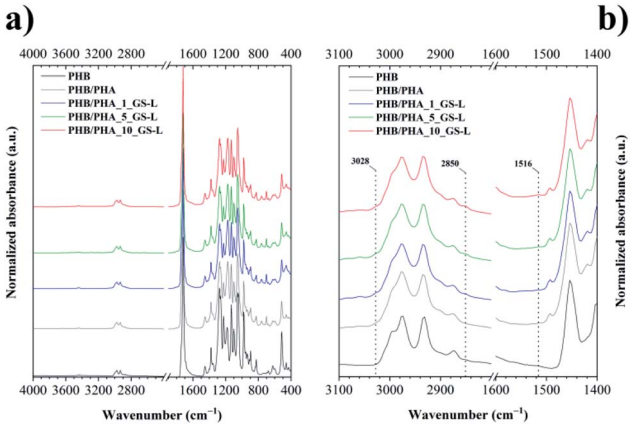

Fig. 4 ATR-FTIR spectra of neat PHB and PHB/PHA blends with or without grape seeds lignin (GS-L), (a) spectral range of 4000–400 cm^{-1} and (b) spectral range of 3100–1400 cm^{-1}.

Table 5 DSC data of PHA pellets, PHB and PHB/PHA films

Sample		1st heating scan		Cooling scan		
		T_m (°C)	ΔH_m (J g^{-1})	T_c (°C)	ΔH_c (J g^{-1})	T_g (°C)
PHA	Pellets	—	—	—	—	26.7
PHB	Film	170.5	87.1	124.0	80.3	nd
PHB/PHA	Film	157.7/171.8	45.5	106.4	42.0	nd
PHB/PHA_1_GS-L	Film	157.6/172.2	46.0	114.4	41.2	nd
PHB/PHA_5_GS-L	Film	170.7	48.0	121.2	41.7	nd
PHB/PHA_10_G-L	Film	168.6	41.0	116.3	35.8	nd

asymmetric and symmetric C–O–C stretching of saturated aliphatic esters. Another significant band occurring at 1261 cm^{-1} is able to assign to symmetric C–O stretching of ester functional groups. Furthermore, the presence of saturated esters was recorded by the band at 1099 cm^{-1}, attributed to asymmetric O–C–C stretching of PHAs. All the films' spectra also contain a sharp and intensive band at 1052 cm^{-1} that corresponds to the stretching of the second C–O bond in the ester groups (*i.e.*, O–C–C). The less intense absorption bands at 2977 cm^{-1} and 2935 cm^{-1} were ascribed to asymmetric and symmetric C–H stretching in –CH_3 functional groups. The bands revealed hydrocarbons at 1454 cm^{-1} and 1381 cm^{-1}, which can be ascribed to the deformation vibrations of methylene and methyl groups.

The presence of lignin characteristic peaks on the surface of blends can be seen in Fig. 4b. The aromatic skeletal vibrations are presented as peaks in the two spectral ranges of 3100–3000 cm^{-1} and 1600–1500 cm^{-1}. All the spectra of PHB/PHA with lignin contained a less intensive shoulder at about 3028 cm^{-1} showing the presence of aromatic rings. The vibration modes of aromatic moieties, which can be attributed to symmetric C=C stretching, occurred in the spectra at 1516 cm^{-1}. Another difference in PHB/PHA films with lignin is the presence of the band and/or shoulder at 2850 cm^{-1}. This band was attributed to the symmetric C–H stretching in –CH_2– functional groups.

3.2.2. Thermal properties. The thermal behaviour of neat PHA films and PHA films modified with grape seeds lignin was studied by non-isothermal DSC experiments. The data of non-isothermal DSC are summarized in Table 5. Fig. 4 shows the first heating and cooling scans. The amorphous PHA employed in this work cannot melt or crystallize; it is an amorphous polymer with the glass transition temperature at −26.7 °C. The amorphous PHA was produced by fermentation and extraction processes patented by former company Metabolix (Cambridge, MA, USA). The inability to crystalize is related to the chemical structure of PHAs; the amorphous PHAs belong to the medium-chain-length (mcl-) PHAs. The advantage of the amorphous PHAs is that these polymers are flexible and their mechanical properties are similar to elastomers.[48] In contrast to amorphous PHAs, poly(3-hydroxybutyrate) (PHB) that belong to the short-chain-length (scl-) PHAs are stiff polymers with a high degree of crystallinity and brittleness. The crystallization behaviour of PHB depends on its molecular weight, additives (*e.g.*, nucleating additives) and polymer processing conditions (heating/cooling).[49,50] It is important to note that the crystalline structure of PHB films produced through solution casting differs in comparison with the materials produced by melt processing, *e.g.*, extrusion or thermoforming. The crystals of solution cast materials have an elongated shape and reminiscent of lath-like polypropylene crystals.[51] Scl-PHAs, including PHB, are semi-crystalline polymers with high degrees of crystallinity. DSC thermograms are displayed in Fig. 5 and thermal data are summarized in Table 5.

Amorphous PHA did not crystallize and showed a glass transition temperature (T_g) at 26.7 °C. Neat PHB displayed a broad melting peak at 170.5 °C with the melting enthalpy of 87.1 J g^{-1}. The PHB film reached the degree of crystallinity of

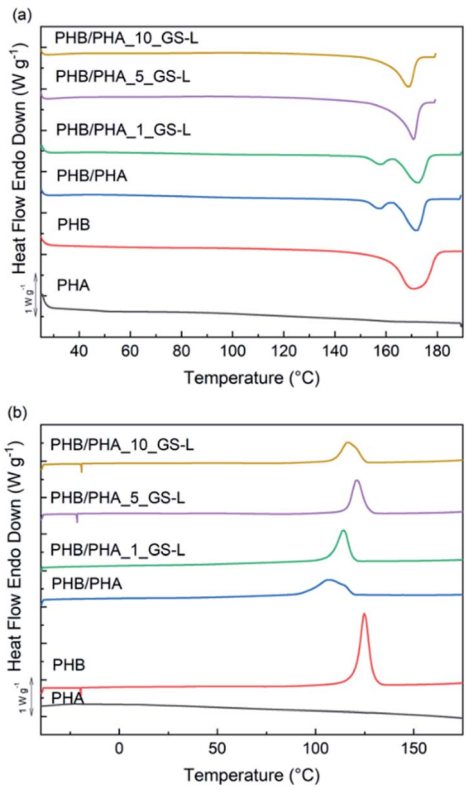

Fig. 5 DSC (a) first heating scans and (b) cooling scans for PHA, PHB, PHB/PHA, PHB/PHA_1_GS-L, PHB/PHA_5_GS-L, and PHB/PHA_10_GS-L.

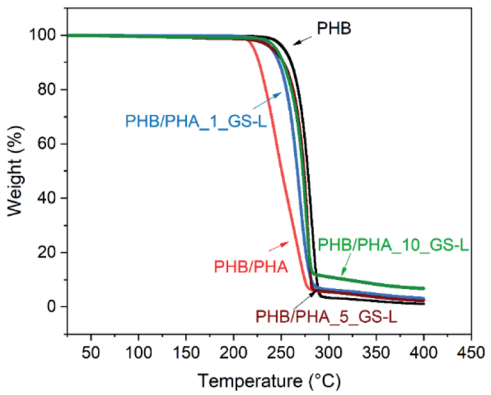

Fig. 6 Weight of the samples as a function of temperature obtained by TGA for PHB and PHB/PHA films.

Table 6 TGA data of PHB and PHB/PHA films in air and at heating rate of 10 °C min^{-1}

Sample	T_{onset} (°C)	T_{max} (°C)	$Mass_{rest}$ at 400 °C (%)
PHB	244.0	281.5	1.0
PHB/PHA	215.5	245.1	2.5
PHB/PHA_1_GS-L	230.6	269.1	3.0
PHB/PHA_5_GS-L	224.8	277.3	2.9
PHB/PHA_10_GS-L	235.7	275.3	6.7

about 59.7% that was such a high value that it was not possible to detect the value of T_g by DSC technique. The melting behaviour of films produced by the blending of PHB with amorphous PHA in the 1 : 1 ratio corresponded with the PHB content. The PHB/PHA film showed a double melting peak and the degree of crystallinity that corresponded to the PHB content (Fig. 5a). The double melting peak at 157.7 °C and 171.8 °C indicates the presence of crystallites with different morphology and thermal stability. Fig. 5b shows that also the crystallization kinetics of the PHB/PHA blend was modified due to the presence of amorphous PHA. The blend crystallized with the lower value of the enthalpy of crystallization and much later than neat PHB.

In our previous works,[52,53] we have presented that lignins as natural phenolic aromatic additives may work as nucleating agents for polyesters. The nucleating efficiency depended on the type of lignin and mainly on its physical and chemical properties that influenced the interfacial compatibility between lignin and polymer matrix. Similarly, the thermal data in this work showed that the GS-L was active as a nucleating agent in the PHB/PHA blend. However, the effect of lignin on PHB/PHA crystallization kinetics depended on its concentration. The highest nucleation effect was manifested at a 5 wt% concentration of lignin. Lower or higher lignin concentrations were not active enough in terms of the crystallization behaviour of the PHB/PHA blend.

The thermal stability of films in the air was determined by thermogravimetry (TGA). Fig. 6 shows the TGA curves of PHB, PHB/PHA and PHB/PHA with GS-L lignin up to 400 °C. The onset of thermal degradation (T_{onset}), the temperature with the maximum sample weight-loss (T_{max}) and the residual mass at 400 °C are reported in Table 6.

Table 7 Mechanical properties of PHB and PHB/PHA films

Sample	E (MPa)	σ_{max} (MPa)	ε_B (%)
PHB	2050 ± 220	49.2 ± 3.5	8.4 ± 1.6
PHB/PHA	240 ± 12	6.6 ± 0.5	95.2 ± 12
PHB/PHA_1_GS-L	302 ± 12	29 ± 0.8	68 ± 20
PHB/PHA_5_GS-L	200 ± 17	36 ± 3.0	82 ± 30
PHB/PHA_10_GS-L	827 ± 60	13 ± 2.0	15 ± 4.0

The values of the onset of thermal degradation showed that neat PHB film was the most stable material since it had the highest value T_{onset} value at 281.5 °C. The higher thermal stability of PHB corresponds with its high degree of crystallinity. The onset of thermal degradation for the PHB/PHA blend started about 28.5 °C earlier. The addition of GS-L lignin markedly shifted T_{onset} as well as T_{max} values to higher temperatures about 9.3–20.2 °C and 24.0–32.2 °C, respectively. The improved thermal stability of blends containing lignin correlates well with the increased degrees of crystallinity of blends. These results correspond with the findings of other authors, who reported that the admixture of lignin in low concentrations contributed to the higher thermal stability of PHB mainly due to the physical barrier effect of lignin.[54,55]

3.2.3. Mechanical properties. Table 7 shows the mechanical properties of neat PHB, PHB/PHA blend and PHB/PHA/GS-L films. The neat PHB films displayed E-modulus of 2050 MPa, tensile stress at a maximum of 49.2 MPa and tensile strain at break of 8.4%. The values of E-modulus and tensile stress at the maximum of PHB/PHA film markedly decreased compared to neat PHB film. Nevertheless, the tensile strain at break values increased by about 86.8%. These changes correspond with the semi-crystalline state and viscoelastic behaviour of PHB and PHB/PHA blend. The mechanical properties of PHB/PHA blends

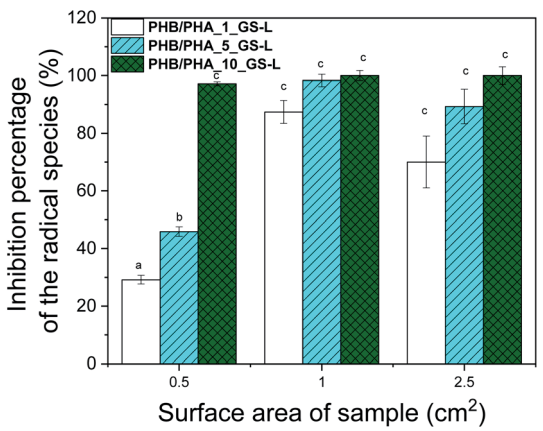

Fig. 7 Antioxidant activity of GS-L lignin in PHB/PHA blend films expressed as inhibition percentage of ABTS radicals. Bars marked by different letters are significantly different ($p < 0.01$).

Table 8 The percentage of grape seed lignin (GS-L) leached from PHB/PHA films after 8 days into 10 w/v% or 50 w/v% aqueous ethanol at 23 °C and 50 rpm

	Lignin migration from the foil (mg dm^{-2})	
Sample	10 w/v% ethanol (v/v)	50 w/v% ethanol (v/v)
PHB/PH_5_GS-L	7.3 ± 0.9	20.5 ± 1.2
PHB/PH_10_GS-L	15.8 ± 1.0	35.0 ± 1.9

with lignin depended on the admixed lignin concentration. Lignin improved the stiffness of the PHB/PHA blend but negatively influenced the tensile strain at break values. The reason for the increase in the stiffness is the aromatic character and reinforcing capacity of lignin. However, this effect is limited by the interfacial adhesion level between lignin and PHB/PHA blend. Five percentage was detected as an optimal concentration to reach good mechanical properties of films. The limited compatibility of lignin with biopolyesters was also reported in other works.[56,57]

3.2.4. Antioxidant capacity of grape seeds lignin in PHB/PHA films. The antioxidant capacity of grape seeds lignin in PHB/PHA films was tested by using ABTS radical scavenging assay. The incorporation of grape seeds lignin into the PHB/PHA blend introduces a radical scavenging functionality in the final films (see Fig. 7).

Using a one-way ANOVA for statistical analysis, a significant radical scavenging activity of grape seeds lignin added in PHB/PHA films, was determined. The inhibition percentage of ABTS radical scavenged increased with lignin concentration and with the area of the tested film. The film's radical scavenging capacity with the surface area of 1 cm^2, containing 1 wt% of lignin, was comparable to the film with the surface area of 0.5 cm^2 having 10% of lignin. The larger surface area means a higher concentration of lignin and higher scavenging activity. The optimal concentration of lignin to reach maximal scavenging capacity is between 1–5 wt%. A similar efficient concentration of lignin was detected in work showing antioxidant effectiveness of pre-hydrolysis lignin incorporated in virgin and recycled polypropylene.[37,58]

3.2.5. Gas permeability and migration of lignin from films. EU Directive 10/2011 limited the overall migration to 10 mg dm^{-2} on a contact area basis or 60 mg kg^{-1} in the simulant or food.[31,59] The determined values of lignin migration into simulants 10 w/v% or 50 w/v% ethanol are shown in Table 8. The lignin migration from the film with 5 wt% lignin in 10 w/v% or 50 w/v% ethanol reached about 7.3 and 20.5 mg dm^{-2}, respectively. The film with the 10 wt% content of lignin released in 10 w/v% or 50 w/v% ethanol, about 15.8 and 35.0 mg dm^{-2}, respectively. The migration limits fulfilled only PHB/PHA film with 5 wt% lignin in simulant that represented the aqueous food products. In conclusion, the higher concentration of lignin in the film meant higher values of migrated lignin into the environment. The increased amounts of released lignin in 50 w/v% ethanol indicated that these packaging films were not suitable for fatty food.

The function of polymer films used as food packaging materials is to protect food from mechanical damage and direct interaction with the environment. Some food packaging applications are required to reach low values of gas permeability (mainly oxygen and carbon dioxide). Gas permeability of polymer films depends on molecular structure, chemical composition and polymer morphology.[60] PHAs have comparable or better gas permeability as conventional non-biodegradable thermoplastics. Therefore, PHAs belong to promising candidates for food packaging applications.[61,62]

The surface morphologies of neat PHB, PHB/PHA blend and PHB/PHA films with one or ten percent of grape seeds lignin were investigated by scanning electron microscopy (Fig. 8). The morphology of PHB/PHA blends differed significantly from pure PHB film. PHB/PHA films contained nanopores probably formed due to the immiscibility of crystalline PHB and amorphous PHA. The addition of 1 wt% or 10 wt% lignin had a minimal effect on the resulting film morphology. Lignin, due to its good solubility in chloroform and compatibility with PHA, is difficult to recognize. The resulting structure of PHB–PHA/GS-L films is only slightly more compact, showing lightly smaller pores sizes in the structure.

All tested PHA films in this work had much lower oxygen and carbon dioxide permeability than polyolefin films (see Table 9). The hypothesis in this work was that grape seeds lignin might contribute to the lower gas permeability of PHA films. In our last work, we have found that methanol kraft lignin incorporated in

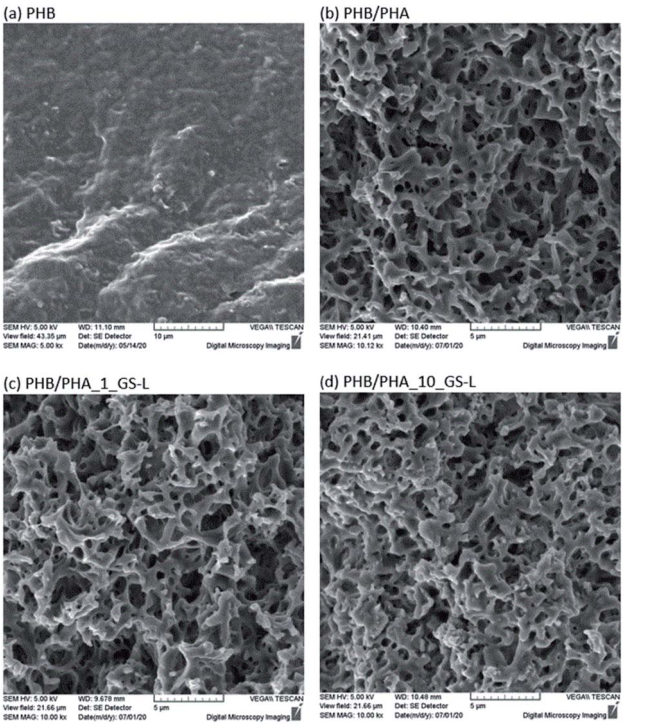

Fig. 8 SEM morphology of neat PHB, PHB/PHA, PHB/PHA_1-GS-L and PHB/PHA_10-GS-L.

Table 9 Oxygen and carbon dioxide transfer rates of polymer films at room temperature. GTR-gas transfer rate

	GTR (cm^3 m^{-2} 24 h 0.1 MPa)		
Sample	Oxygen	Carbon dioxide	Reference
PHB/PHA	19.0	191.4	(This work)
PHB/PHA_1_GS-L	7.3	36.3	(This work)
PHB/PHA_10_GS_L	6.1	4.0	(This work)
PHB	20.9	52.8	63
PHBV	4.9–16.5	127.4–144.0	53 and 64
PP	79.5–104.0	267.0–322.3	65
PE	100.7–400	789.5	64
HDPE with 3 bilayers	73.2	—	66
HDPE with 5 bilayers	10.6	—	64

poly(3-hydroxybutyrate-*co*-3-hydroxyvalerate) (PHBV) improved the gas barrier of PHBV films.[53] However, the efficiency of lignin depends on its interfacial adhesion with the polymer matrix. Therefore the activity of a specific type of lignin can not be generalized on all lignin types. The gas transfer rates data (GTR) of PHB/PHA films are displayed in Table 9.

The data show that the blending of PHB with an amorphous PHA increased the permeability of carbon dioxide at least about 260%. The reason for lower gas barrier efficiency of PHB/PHA film compared to neat PHB can be the plasticizing effect of the amorphous PHA. The oxygen permeability of PHB/PHA films is comparable with neat PHB. The incorporation of grape seeds lignin into PHB/PHA improved the gas barrier function of films. The GTR data for O_2 and CO_2 markedly decreased with 1 or 10 wt% of grape seeds lignin. The gas barrier functionality of films was improved due to the new reinforced surface morphology, which limits the transport of O_2 and CO_2 molecules.

3.2.6. Biodegradation and phytotoxicity. The advantage of PHA-based packaging materials is their biodegradability. However, the addition of lignin could change this advantage. Lignin is composed mostly of carbon, hydrogen and oxygen, which are elements that are not harmful to the environment. However, it is known that white-rot fungi can only biodegrade lignin.[67] Therefore, the effect of lignin on the biodegradation process of PHA films was investigated in this work.

Gradually, with the degradation of polyhydroxyalkanoates, the soil's pH was changing, and the value at the end of the composting process was 5.5. The ambient temperature during the experiment was maintained at 58.3 °C. Changes in temperature profile occurred due to soil mixing and aeration. Odour monitoring showed that acid and ammonia were developed within the first 14 days. Later, the compost fillings did not release any unwanted or unpleasant odours and at the end of the experiment, the compost smelled quite pleasantly like topsoil. At the end of the composting period, the obtained sample fragments showed colour and shape changes. The detailed records of pH and temperature monitoring and photographs of the recovered fragments of films at the end of the composting experiment are shown in the ESI (see Fig. S4 and S5).†

Table 10 Weight changes in PHA films after composting and degradability degree (*D*)

Sample	m_E[a] (g)	(*D*) degradability degree (%)
PHB	0.85	42.18
PHB/PHA	0.50	68.75
PHB/PHA_1_GS-L	0.27	83.63
PHB/PHA_5_GS-L	0.75	55.62
PHB/PHA_10_GS-L	0.44	75.69
Reference (filter paper)	0.15	85.00

[a] m_E represents the dry mass of the recovered material after.

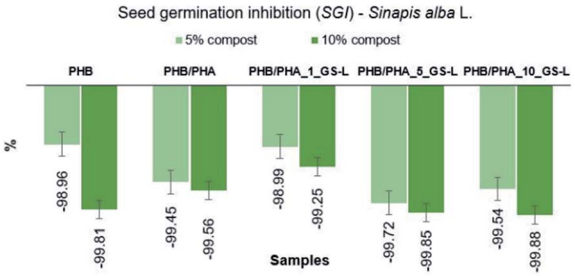

Fig. 9 Seed germination inhibition test of PHB, PHB/PHA, PHB/PHA_1_GS-L, PHB/PHA_5_GS-L, and PHB/PHA_10_GS-L films.

The recorded dry mass and degradability degrees (*D*) of PHA films are listed in Table 10. The degradability degree of the reference reached more than 80%, confirming the success and validity of the composting test. The recorded degradability degree values showed that admixture of 50 wt% amorphous PHA to crystalline PHB improved biodegradation of films about 26.6%. The degradability degree of the PHB/PHA film was changed after the addition of lignin. The addition of 1 wt% and 10 wt% of lignin promoted biodegradation about 7.9–14.9%. In contrast, the addition of 5 wt% lignin reduced the degree of degradability of the PHB/PHA_5_GS-L film, about 13.1% compared to neat PHB/PHA film. The lower degree of degradability may be related to the high antioxidant activity of the PHB/PHA_5_GS-L film.

To predict the effects of PHA films on seed germination, the seed germination inhibition (SGI) was estimated for white mustard (*Sinapis alba* L.) cultivated in soil mixed with the compost material after biodegradation of PHA films. Materials with SGI values higher than zero indicate seed germination inhibition and the SGI values higher than ten show soil toxicity. While SGI values, which are lower than zero, indicate the stimulation effect of soil. The determined percentages of SGI are displayed in Fig. 9.

The obtained SGI values in the range from −98.96% to −99.88% confirmed the nontoxicity of all tested polyhydroxyalkanoates with or without lignin. These results even showed the highly stimulating effect of compost obtained after biodegradation of PHA films on the seed germination and

growth of white mustard (*Sinapis alba* L.) All tested composts exhibited high stimulating effects (SGI < 0). In samples with the 5% content of tested composts, SGI ranged from −98.96% to −99.72%. Samples with 10% of tested composts exhibited even higher stimulating effects ranging from −99.25% to −99.88%.

4. Conclusions

In this work, the effectivity of lignin isolated from grape seeds as the radical scavenging additive for polyhydroxyalkanoates has been studied. PHB/PHA films were prepared *via* solution casting in chloroform. The ductility of poly(3-hydroxybutyrate) has been markedly improved by blending with amorphous polyhydroxyalkanoate. However, the thermal stability of the PHB/PHA blend compared to neat PHB decreased. The onset of thermal degradation under the air environment of the PHB/PHA blend was about 28.5 °C lower compared to neat PHB. The addition of grape seed lignin markedly improved the thermal stability of the PHB/PHA blend.

The grape seed lignin proved to be an effective antioxidant even after addition to the PHB/PHA film. Besides, it acted as a nucleating agent. Therefore, on the one hand, it increased the degree of crystallinity and stiffness of the film and, on the other hand, contributed to the lower oxygen and carbon dioxide permeability of films. The optimal concentration of lignin was in the range of 1–5 wt%.

The ability of PHB/PHA films containing lignin to degrade in compost was confirmed. Moreover, it was found that the biomass obtained after the composting period was able to stimulate the germination of white mustard (*Sinapis alba* L.). To the best of our knowledge, the information that biomass obtained after degradation of polyhydroxyalkanoates with or without lignin can positively stimulate plant growth has not yet been reported in the literature. These results illustrate that the PHB/PHA/GS-L films may expand the applicability of polyhydroxyalkanoates in food packaging as bioactive biodegradable films showing a high radical scavenging activity.

The material properties, the biodegradation and non-phytotoxicity results showed that PHA/PHB films containing grape seeds lignin would not pollute the environment after the termination of their service life.

Conflicts of interest

There are no conflicts to declare.

Acknowledgements

This work was funded through the project SoMoPro (project no. 6SA18032). This project has received funding from the European Union's Horizon 2020 Research and Innovation Programme under the Marie Skłodowska-Curie, and it is co-financed by the South Moravian Region under grant agreement no. 665860. Note: Authors confirm that the content of this work reflects only the author's view and that the EU is not responsible for any use that may be made of the information it contains. The author, Michal Machovsky, also appreciates support from the project "Centre of Polymer System plus" funded by the Ministry of Education, Youth and Sports of the Czech Republic – Program NPU I (project number: LO1504).

References

1 J. Poole, *Packaging trends*, http://www.packaginginsights.com.
2 W. Ker, Y. K. Sen and S. D. Rajendran, *E3S Web Conf.*, 2019, **136**(4), 04092.
3 M. Koller, *Molecules*, 2018, **23**, 362.
4 M. Koller, A. Salerno and G. Braunegg, in *Bio-based plastics: materials and applications*, ed. S. Kabasci, John Wiley & Sons, 2013, pp. 137–169.
5 B. S. T. Gadgil, N. Killi and G. V. Rathna, *MedChemComm*, 2017, **8**, 1774–1787.
6 A. Barrett, *Bioplastics News*, October 15, 2018, https://bioplasticsnews.com.
7 A. Kovalcik, S. Obruca, I. Fritz and I. Marova, *BioResources*, 2019, **14**, 2468–2471.
8 I. Marova, R. Pavelkova, V. Kundrat, P. Matouskova, A. Kovalcik and J. Bokrova, *J. Biotechnol.*, 2019, **305**, S5.
9 S. W. Kim, P. Kim, H. S. Lee and J. H. Kim, *Biotechnol. Lett.*, 1996, **18**, 25–30.
10 S. Obruca, I. Marova, O. Snajdar, L. Mravcova and Z. Svoboda, *Biotechnol. Lett.*, 2010, **32**, 1925–1932.
11 J. C. C. Yeo, J. K. Muiruri, W. Thitsartarn, Z. Li and C. He, *Mater. Sci. Eng., C*, 2018, **92**, 1092–1116.
12 W. B. De Almeida, P. S. Bizzarri, A. S. Durao and J. F. D. Nascimenti, DE602004027554D1, 2010.
13 R. Crétois, J.-M. Chenal, N. Sheibat-Othman, A. Monnier, C. Martin, O. Astruz, R. Kurusu and N. R. Demarquette, *Polymer*, 2016, **102**, 176–182.
14 D. Garcia-Garcia, J. Ferri, T. Boronat, J. López-Martínez and R. Balart, *Polym. Bull.*, 2016, **73**, 3333–3350.
15 M. Wada, H. Kido, K. Ohyama, T. Ichibangase, N. Kishikawa, Y. Ohba, M. N. Nakashima, N. Kuroda and K. Nakashima, *Food Chem.*, 2007, **101**, 980–986.
16 J. Pospíšil, *Polym. Degrad. Stab.*, 1988, **20**, 181–202; M. Wada, H. Kido, K. Ohyama, T. Ichibangase, N. Kishikawa, Y. Ohba, M. N. Nakashima, N. Kuroda and K. Nakashima, *Food Chem.*, 2007, **101**, 980–986.
17 B. Kosikova, J. Labaj, A. Gregorova and D. Slamenova, *Holzforschung*, 2006, **60**, 166–202.
18 V. Siracusa, P. Rocculi, S. Romani and M. D. Rosa, *Trends Food Sci. Technol.*, 2008, **19**, 634–643.
19 B. Laycock, M. Nikolić, J. M. Colwell, E. Gauthier, P. Halley, S. Bottle and G. George, *Prog. Polym. Sci.*, 2017, **71**, 144–189.
20 Tappi Standards, *Acid-insoluble lignin in wood and pulp, Tappi Method T 222 om-06*, Tappi Press, Atlanta, GA, 2006.
21 Tappi Standards, *Acid-soluble lignin in wood and pulp, Tappi Method UM 250*, Tappi Press, Atlanta GA, 1985.
22 Y.-W. Wang, Q. Wu and G.-Q. Chen, *Biomaterials*, 2003, **24**, 4621–4629.
23 W. G. Glasser, V. Davé and C. E. Frazier, *J. Wood Chem. Technol.*, 1993, **13**, 545–559.
24 S. A. Contreras, A. R. Gaspar, A. Guerra, L. A. Lucia and D. S. Argyropoulos, *Biomacromolecules*, 2008, **9**, 3362–3369.

25 G. Zinovyev, I. Sulaeva, S. Podzimek, D. Rössner, I. Kilpeläinen, I. Sumerskii, T. Rosenau and A. Potthast, *ChemSusChem*, 2018, **11**, 3259–3268.
26 O. Gordobil, R. Herrera, M. Yahyaoui, S. Ilk, M. Kaya and J. Labidi, *RSC Adv.*, 2018, **8**, 24525–24533.
27 S. S. Qazi, D. Li, C. Briens, F. Berruti and M. M. Abou-Zaid, *Molecules*, 2017, **22**(372), 1–14.
28 R. Re, N. Pellegrini, A. Proteggente, A. Pannala, M. Yang and C. Rice-Evans, *Free Radicals Biol. Med.*, 1999, **26**, 1231–1237.
29 K. J. Olejar, S. Ray, A. Ricci and P. A. Kilmartin, *Cellulose*, 2014, **21**, 4545–4556.
30 A. Arshanitsa, J. Ponomarenko, T. Dizhibite, A. Andersone, R. J. A. Gosselink, J. van der Putten, M. Lauberts and G. Telysheva, *J. Anal. Appl. Pyrolysis*, 2013, **103**, 78–85.
31 K. Bhunia, S. S. Sablani, J. Tang and B. Rasco, *Compr. Rev. Food Sci. Food Saf.*, 2013, **12**, 523–545.
32 M. Vaverková, F. Toman, D. Adamcová and J. Kotovicová, *Ecol. Chem. Eng. S*, 2012, **19**, 347–358.
33 D. Adamcová, M. D. Vaverková and E. Břoušková, *J. Ecol. Eng.*, 2016, **17**, 33–37.
34 C. Valiente, E. Arrigoni, R. M. Esteban and R. Amado, *J. Food Sci.*, 1995, **60**, 818–820.
35 F. M. Yedro, J. Garcia-Serna, D. A. Cantero, F. Sobrón and M. J. Cocero, *RSC Adv.*, 2014, **4**, 30332–30339.
36 B. Košíková, V. Demianova and M. Kačuráková, *J. Appl. Polym. Sci.*, 1993, **47**, 1065–1073.
37 A. Gregorova, Z. Cibulkova, B. Kosikova and P. Simon, *Polym. Degrad. Stab.*, 2005, **89**, 553–558.
38 A. Gregorova, B. Kosikova and R. Moravcik, *Polym. Degrad. Stab.*, 2005, **91**, 229–233.
39 I. Šurina, M. Jablonský, A. Ház, A. Sladková, A. Briškárová, F. Kačík and J. Šima, *BioResources*, 2015, **10**, 1408–1423.
40 J. Lora, in *Monomers, Polymers and Composites from Renewable Resources*, ed. M. N. Belgacem and A. Gandini, Elsevier Science, Amsterdam, 2008, pp. 225–242.
41 A. Brandt, L. Chen, B. E. van Dongen, T. Welton and J. P. Hallett, *Green Chem.*, 2015, **17**, 5019–5034.
42 V. M. Roberts, V. Stein, T. Reiner, A. Lemonidou, X. Li and J. A. Lercher, *Chem.–Eur. J.*, 2011, **17**, 5939–5948.
43 J. Sameni, S. Krigstin and M. Sain, *BioResources*, 2017, **12**, 1548–1565.
44 B. H. Stuart, *Infrared Spectroscopy: Fundamentals and Applications*, John Wiley & Sons, Hoboken, 1st edn, 2004.
45 J. Xu, B.-H. Guo, R. Yang, Q. Wu, G.-Q. Chen and Z.-M. Zhang, *Polymer*, 2002, **43**, 6893–6899.
46 J. W. A. Herrera-Kao, M. I. Loría-Bastarrachea, Y. Pérez-Padilla, J. V. Cauich-Rodríguez, H. Vázquez-Torres and J. M. Cervantes-Uc, *Polym. Bull.*, 2018, **75**, 4191–4205.
47 A. Kovalcik, S. Obruca, M. Kalina, M. Machovsky, V. Enev, M. Jakesova, M. Sobkova and I. Marova, *Materials*, 2020, **13**, 1–21.
48 F. Pappalardo, M. Fragalà, P. G. Mineo, A. Damigella, A. F. Catara, R. Palmeri and A. Rescifina, *Int. J. Biol. Macromol.*, 2014, **65**, 89–96.
49 A. Kovalcik, K. Meixner, M. Mihalic, W. Zeilinger, I. Fritz, P. Kucharczyk, F. Stelzer and B. Drosg, *Int. J. Biol. Macromol.*, 2017, **102**, 497–504.
50 A. Gregorova, R. Wimmer, M. Hrabalova, M. Koller, T. Ters and N. Mundigler, *Holzforschung*, 2009, **63**, 565–570.
51 P. Barham, A. Keller, E. Otun and P. Holmes, *J. Mater. Sci.*, 1984, **19**, 2781–2794.
52 A. Kovalcik, R. A. Pérez-Camargo, C. Fürst, P. Kucharczyk and A. J. Müller, *Polym. Degrad. Stab.*, 2017, **142**, 244–254.
53 A. Kovalcik, M. Machovsky, Z. Kozakova and M. Koller, *React. Funct. Polym.*, 2015, **94**, 25–34.
54 P. Mousavioun, G. A. George and W. O. S. Doherty, *Polym. Degrad. Stab.*, 2012, **97**, 1114–1122.
55 F. Bertini, M. Canetti, A. Cacciamani, G. Elegir, M. Orlandi and L. Zoia, *Polym. Degrad. Stab.*, 2012, **97**, 1979–1987.
56 O. Gordobil, I. Egüés, R. Llano-Ponte and J. Labidi, *Polym. Degrad. Stab.*, 2014, **108**, 330–338.
57 O. Gordobil, R. Delucis, I. Egüés and J. Labidi, *Ind. Crops Prod.*, 2015, **72**, 46–53.
58 A. Gregorova, B. Kosikova and A. Stasko, *J. Appl. Polym. Sci.*, 2007, **106**, 1626–1631.
59 Commission Regulation (EU), No. 10/2011, 14 January 2011, http://eur-lex.europa.eu/legal-content/EN/TXT/?uri=OJ:L:2011:012, TOC.
60 R. J. Hernandez and J. R. Giacin, in *Food Storage Stability*, ed. I. A. Taub and R. P. Singh, CRC Press, New York, USA, 1998, Ch. 10, p. 297.
61 L. P. Amaro, M. A. Abdelwahab, A. Morelli, F. Chielini and E. Chielini, in *Recent Advances in Biotechnology. Microbial Biopolyester Production, Performance and Processing. Bioengineering, Characterization, and Suistainability*, ed. M. Koller, Bentham eBooks imprint, 2016, Ch. 1, p. 12.
62 D. Brown and C. Viney, in *Biotechnology. The Science and the Business*, ed. V. Moses, R. E. Cape and D. G. Springham, CRC Press, New York, 1999, Ch, 19, p. 358.
63 V. Siracusa, C. Ingrao, S. G. Karpova, A. A. Olkhov and A. L. Iordanskii, *Eur. Polym. J.*, 2017, **91**, 149–161.
64 G. Keskin, G. Kızıl, M. Bechelany, C. Pochat-Bohatier and M. Öner, *Pure Appl. Chem.*, 2017, **89**, 1841–1848.
65 V. Siracusa, I. Blanco, S. Romani, U. Tylewicz and M. Dalla Rosa, *J. Food Sci.*, 2012, **77**, E264–E272.
66 C. F. Ayuso, A. A. Agüero, J. A. P. Hernández, A. B. Santoyo and E. G. Gómez, *Polym. Polym. Compos.*, 2017, **25**, 571–582.
67 I. D. Reid, *Can. J. Bot.*, 1995, **73**(S1), 1011–1018.